

## Deflecting danger: The role of screen angles in fish impingement

Guglielmo Sonnino Sorisio<sup>a,b,\*</sup>, Charlotte Robison-Smith<sup>b</sup>, Andy Don<sup>c</sup>, Jo Cable<sup>b</sup>, Catherine A.M.E. Wilson<sup>a</sup>

<sup>a</sup> School of Engineering and Water Research Institute, Cardiff University, CF24 3AA, UK

<sup>b</sup> School of Biosciences and Water Research Institute, Cardiff University, CF10 3AX, UK

<sup>c</sup> Environment Agency, Bridgewater, Rivers House, TA6 4YS, UK

### ARTICLE INFO

#### Keywords:

Fish screen  
European eel  
*Anguilla anguilla*  
Impingement  
Entrainment  
Fish Bypass

### ABSTRACT

Water abstractions in inland watercourses have the potential to harm European eel populations (*Anguilla anguilla*) if they are not correctly protected, potentially contributing to further declines of this critically endangered species. Current guidance aim to prevent eel impingement and entrainment at intakes and outfalls by specifying mitigation screening techniques such as screen types, screen apertures, and maximum approach velocities to the screens. These aim to prevent eels from being injured and allow them to bypass the abstraction, but they have yet to be empirically tested. In this study, screens with 3 mm apertures of horizontal and vertical wedge-wire and a Hydrolox screen were evaluated under the current Environment Agency's screening guidance document that supports the Eels (England and Wales) Regulations 2009. We measured the hydrodynamics of the screens and then observed eel behaviour and swimming dynamics upstream of the screens. The screens had minor effects on the upstream flow fields and produced suitable velocities and turbulence levels for eel escapement. At the regulation velocities, no eels impinged on the screens, validating the current guidance but impingement started to occur at higher velocities, so the guidance velocities should not be exceeded. Screens at smaller angles to the flow caused few eel impingements and therefore are preferable. The current screen guidance for 3 mm wedge-wire screens are appropriate for eels of the size tested in this study and do not cause impingement or entrainment.

### 1. Introduction

Water is a limited, diminishing but heavily abstracted resource, with a significant portion, 87 % in England and 73 % in Wales, abstracted from freshwaters (Holleran, 2023; NRW, 2024). In these countries, there are an estimated 17,100 abstraction licences from surface waters (DEFRA, 2022; NRW, 2024), which removed 10.4 billion cubic metres of water in 2018 with a potential increase to 12.7 billion cubic metres in 2023 (DEFRA, 2022; Holleran, 2023; NRW, 2024). The main abstractors of water are from electricity generation and public water suppliers, followed by agriculture, aquaculture, and other industries (Holleran, 2023; NRW, 2024). Such abstractions have the potential to entrain fish (Turnpenny and O'Keefe, 2005) causing them delays at best and death at worst (Carr and Whoriskey, 2008; Carter and Reader, 2000; Dainys et al., 2018; Larinier and Travade, 2002). These abstractions add to the millions of barriers already fragmenting the rivers of Europe and

blocking fish migration pathways (Belletti et al., 2020; Jones et al., 2019). Fish screens are typically employed to mitigate these risks but a poorly designed screen can still cause entrainment for some fish and impingement for others (Bromley et al., 2013; Haddington et al., 1992; Hanson et al., 1977; Seaby, 2023; Turnpenny and O'Keefe, 2005).

The European eel (*Anguilla anguilla*) is a catadromous fish that migrates upstream from the sea into Europe's rivers. It is currently classified as critically endangered (Jacoby and Gollock, 2015; Pike et al., 2020), having undergone four decades of dramatic recruitment decline, now <5 % of pre-1980 levels (Dekker, 2003; ICES, 2020). This decline is caused by a variety of factors, including river fragmentation and the associated deaths and migration delays (Halvorsen et al., 2020; Piper et al., 2017, 2018; Warren and Pardew, 1998). This is exacerbated by the high prevalence of the parasite *Anguillicola crassus* which affects eel swimming behaviour (Kirk, 2003; Newbold et al., 2015) probably making migration barriers harder to overcome (Newbold et al., 2015).

\* Corresponding author at: School of Engineering and Water Research Institute, Cardiff University, CF24 3AA, UK.

E-mail addresses: [SonninoSorisioG@cardiff.ac.uk](mailto:SonninoSorisioG@cardiff.ac.uk) (G. Sonnino Sorisio), [Robison-SmithCA@cardiff.ac.uk](mailto:Robison-SmithCA@cardiff.ac.uk) (C. Robison-Smith), [andy.don@environment-agency.gov.uk](mailto:andy.don@environment-agency.gov.uk) (A. Don), [CableJ@cardiff.ac.uk](mailto:CableJ@cardiff.ac.uk) (J. Cable), [WilsonCA@cardiff.ac.uk](mailto:WilsonCA@cardiff.ac.uk) (C.A.M.E. Wilson).

<https://doi.org/10.1016/j.ecoleng.2025.107547>

Received 9 October 2024; Received in revised form 17 January 2025; Accepted 5 February 2025

Available online 15 February 2025

0925-8574/© 2025 The Authors. Published by Elsevier B.V. This is an open access article under the CC BY license (<http://creativecommons.org/licenses/by/4.0/>).

Juvenile eels are especially vulnerable because they have a low swimming performance (Clough et al., 2004; Clough and Turnpenny, 2001; Turnpenny et al., 2001; Veza et al., 2020), and are therefore more likely to go through the screen, known as entrainment, if the aperture is large, or impinge on the screen if it is small.

Following the 2007 European Union Eel Regulation (Council Regulation EC No 1100/2007, 2007) and the subsequent UK application of this into England and Wales (The Eels (England and Wales) Regulations 2009 No. 3344, 2009), the European eel is protected in its migrations. This guidance stipulates a target of 40 % biomass escapement of eels to the sea, measured relative to escapement in an unmodified and healthy catchment. Efficient screening techniques can reduce mortalities and help to achieve the required escapement levels, but screening guidance must balance several practical challenges. The screen aperture should prevent entrainment, the approach velocities should not cause impingement, the screen material should not cause injury to the fish, and the screen must achieve this whilst allowing the required volume of water through without being prohibitively expensive. Current Environment Agency (2020) guidelines define Best Achievable Eel Protection (BAEP) as the standard for eel protection at intakes and specify the allowable range of screen aperture, approach velocity, and angles for each size range of fish. For eels 121–300 mm long, approach velocities of  $0.15 \text{ ms}^{-1}$  for screens at  $90^\circ$  and  $31.5^\circ$ , and  $0.3 \text{ ms}^{-1}$  for screens at  $26.5^\circ$  and  $20^\circ$  are recommended (Environment Agency, 2020).

Several screening techniques and guidelines have been developed to increase the efficiency of fish escapement. For most species, screen aperture should be around 10 % of the fish's length to exclude them, however because of the eel's elongated body, the recommended size is 3 % of their length (David et al., 2022; Ebel, 2016). For eels 60–80 mm and 100–160 mm long, respective 1 mm and 2 mm apertures cause no entrainment (Carter et al., 2023), but for silver eels ( $\sim 660 \text{ mm}$ ), 12 mm (Russon et al., 2010), and 15 mm (David et al., 2022) apertures are effective. Apertures up to 30 mm can also function to guide eels to bypasses (Meister, 2020; Motyka et al., 2024), but this aperture does not guarantee exclusion and behavioural screening techniques have been used to supplement the physical screen. Electrification of bar racks causes avoidance but can cause injuries and some eels still entrain (Meister, 2020). Acoustic and infrasound deterrents marginally increased avoidance but the effect was small (Deleau et al., 2020a, 2020b; Piper et al., 2019). Light-based deterrents show the most promise for eels (Haddingth et al., 1992), but efficiency differs amongst species and fish ages. The screen material must be an appropriate balance of fish protection, hydraulic performance, and cost. Bar racks orientated vertically or horizontally are a widespread solution (de Bie et al., 2021; Lemkecher et al., 2022; Meister, 2020; Meister et al., 2020b), larger apertures are usually used, but round bars are prone to 'gill' fish (Turnpenny and O'Keefe, 2005). A variation of this design is foil shaped bars, designed to reduce head losses from the screen (Meister et al., 2020a). Wire mesh and perforated plates can easily clog and be hard to clean, whereas wedge wire screens (Fig. 1) present a smooth surface to the fish and are less prone to debris accumulation whilst also decreasing the blocked area within the screen due to their triangular profile, which does not compromise rigidity (Bromley et al., 2013; Turnpenny and O'Keefe, 2005).

The orientation of the screening material (referred hereafter as vertical or horizontal) is often linked to the axis on which the screen is angled and the location of the bypasses such that the screening material guides towards the bypass. Vertical screens are often the preferred orientation if inclined with respect to the bed and guide to a surface bypass (David et al., 2022; Raynal et al., 2013). However, a vertical or horizontal screen can be positioned across the river channel at an angle to the main flow direction and this is the more common approach, and often leads to a fish bypass at the downstream end of the screen (David et al., 2022; de Bie et al., 2018; Harbicht et al., 2022; Meister, 2020; Motyka et al., 2024) or in rare cases located at the upstream end (Russon et al., 2010). Flume studies with screens directly perpendicular to the

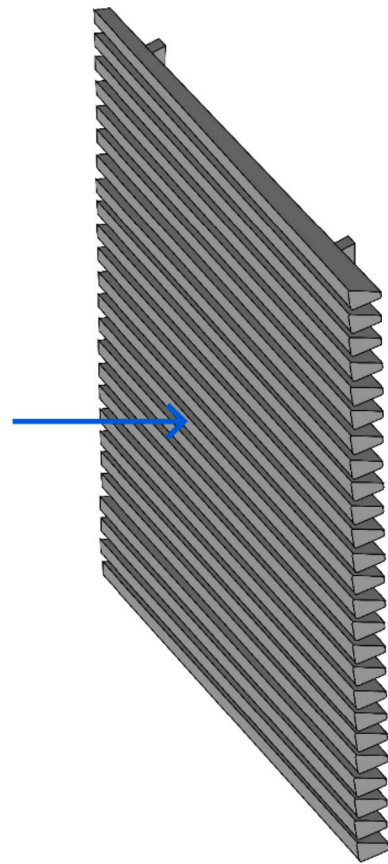


**Fig. 1.** An illustration of a Wedge Wire screen oriented horizontally. In the present study, the Wedge Wire made from stainless steel was 3 mm thick with 3 mm gaps between each bar. Flow direction in this diagram is indicated by the blue arrow with the thicker section of the wedge wire on the upstream face and the tapered trailing end on the downstream face. (For interpretation of the references to colour in this figure legend, the reader is referred to the web version of this article.)

flow direction show high impingement rates and less efficient guidance towards the bypass (Carter et al., 2023; Russon et al., 2010), whereas angled screens have a greater ability to guide fish. Comparing vertical and horizontal screens, some studies on fish species other than eels have found horizontal screens were up to 20 % more effective for guidance, whereas others found little difference (de Bie et al., 2018, 2021; Harbicht et al., 2022). The location and type of bypass has a large impact on the overall effectiveness of installation; a badly designed bypass can delay migrating eels by days, weeks, or months (Behrmann-Godel and Eckmann, 2003; Brown and Castro-Santos, 2009; Carr and Whoriskey, 2008; Gosset et al., 2005; Haro et al., 2000; Pedersen et al., 2012). Juvenile eels primarily swim near the bed, and this is also true in the presence of fish screens (Russon et al., 2010). Surface and pipe bypasses for fish have consequently been found to be a poor design for eels, with down to 0 % passage (Boes et al., 2022; Calles et al., 2012; Egg et al., 2017), and bottom bypasses are generally preferred (Calles et al., 2012; Egg et al., 2017; Environment Agency, 2020). Full depth bypasses have the best passage rates in flume trials but are not always practical in the field (Boes et al., 2022; Harbicht et al., 2022; Russon et al., 2010). Passage rate is also influenced by other factors; flowrate, should be 2–5 % of the total flow (Environment Agency, 2020), and velocity gradient should be mild to attract the eels without being too high and abrupt as this can cause rejections (Boes et al., 2022; de Bie et al., 2018; Piper et al., 2015). More specifically, a 20 % velocity increase towards a bypass increased passage whereas a 40 % increase decreased it (Beck et al., 2020a, 2020b). Variables external to screen design can also

influence eel behaviour and passage rates, low dissolved oxygen levels are associated with higher impingement rates (Shepherd et al., 2016), temperature affects fish swimming abilities (Clough et al., 2004; Muhawenimana et al., 2021), and silver eel body mass has been linked to passage success (Motyka et al., 2024).

Approach velocity to the screen can significantly impact impingement and is fish species and life stage specific, therefore it needs to be low enough for the weakest swimmer (Russon et al., 2010; Stocks et al., 2019). For juvenile eels, for example, 0.2 m/s caused up to 100 % impingement rates (Carter et al., 2023). Another important parameter to consider is how fish screens affect the flow, potentially impacting both the abstraction and the fish. With any blockage of the flow, there will be a loss of velocity head. The most influential parameters on head loss for horizontal bar racks are screen angle, where a low angle to the flow direction creates a lower head (Lemkecher et al., 2022), and bar opening (Albayrak et al., 2020), while the bar shape had less significant effects (Meister, 2020). In terms of the local flow field, the effect of screens on the upstream velocity profile is small compared to the change in the main component of velocity, and a sweeping flow component is generated along the screen surface bar, but orientation did not significantly affect this (Beck et al., 2020a; Lemkecher et al., 2018, 2022; Meister et al., 2020b; Rajaratnam et al., 2010) while screen angle does have an effect on sweeping flow (Albayrak et al., 2020).

At present, most studies evaluating screening technology for eels have concentrated on the seaward migration of the silver eel and there is little evidence available for the best screening approaches to protect elvers and yellow eels. In particular, screen orientation and angle have yet to be evaluated for the current set of UK Environment Agency (2020) guidance. So here we test eel responses to different screen angles, flow velocity, and bypass type. As the effect of screen angle on velocity profile for Wedge Wire Screens angled to the main flow direction (but not the bed) has yet to be experimentally evaluated, we conduct here a hydrodynamic investigation which can be utilised to validate the results of previous Computational Fluid Dynamics (CFD) studies. The effect that screen angle has on impingement is also poorly understood; steeper angles can reduce impingement, and the current guidance allow higher approach velocities at angles below 26.5° to the longitudinal flow direction, but the underlying mechanisms of impingement are unknown. This study, therefore, aims to collect data on impingement rates for juvenile eels at a range of screen angles and flow velocities for horizontal and vertical screen bar orientations and to test three bypass types in conjunction with screen angle. Eel swimming kinematics will be evaluated to provide further details of eel interactions with the screens and this data will be combined with hydrodynamic data to gain a better understanding of fish screen behaviour.

## 2. Methods

### 2.1. Fish origin and maintenance

European eels, *Anguilla anguilla* ( $N = 32$ ), were collected from the River Taff downstream of Blackweir (51.495050, -3.195827) on 22/06/2023, by electrofishing conducted by Natural Resources Wales (NRW). The eels were transported to Cardiff School of Engineering and acclimatised to the holding tank temperature (17 °C) at a rate of 2 °C/h. The holding tank was 1.3 m in diameter with a water depth of 0.35 m, giving a volume of 460 L. The tank contained water dechlorinated with Tetra Aquasafe and filtered and cooled through a Aquamanta EFX 600 External Canister Filter and D—D Aquarium Solution DC 750 connected in series (at a flowrate of approximately 0.75 Ls<sup>-1</sup>). The tank was provided with tubes and rocks to create refugia for the eels and an automatic light kept a 16:8 h light:dark cycle in keeping with the sunlight hours at the time of the experiment. The fish were fed bloodworm daily each morning before the trials and the water quality was checked every other day to ensure that pH, ammonia and nitrites were in the recommended margins (ammonia 0–0.2 mg/L; nitrite 0–0.25 mg/L; and pH

7–8). The tank was kept shut with a plexiglass sheet to ensure no eels were able to escape. Fish size averaged 168 mm in keeping with the specific section of the eel screen guidance being tested, for full measurement details, see Table 1 in the supplementary materials. After the trials were completed, all eels were measured with calipers from the tip of the head to the tip of the tail and weighed, then returned to the location of their capture. All work was approved by Cardiff University Animal Ethics Committee and linked to UK Home Office PP816714.

### 2.2. Experimental setup

The trials were conducted in an open channel recirculating flume 10 m long, 1.2 m wide and 0.3 m deep with a bedslope of 1/1000. The experimental area consisted of a screen mounted at either 90°, 31.5°, 26.5°, or 20° to the flow direction (Fig. 2), and 4 m upstream of the screen left with a bare flume bed (PVC) and walls (glass). At the upstream end of the flume and downstream of the fish screen, flow straighteners were used to prevent the eels from escaping the designated area. The screens were attached to the flume walls with G clamps and sections of screen were joined together by G clamps and zip ties to produce different screen lengths to achieve the correct screen length for the angle required. When a bypass was present, a 130 mm wide gap was left at the downstream end of the screen between the screen and the wall, and the screen was then supported by a wooden arm attached to the flume wall and screen end. For a full depth bypass, the gap was left unobstructed whereas for surface and bottom bypasses, a blanking plate was used to block the bottom and top half of the flow depth respectively. Attention was taken to never leave gaps between screen sections or the walls or bed and to present a smooth screen surface. Three screen types were tested, horizontal and vertical wedge wire screens with 3 mm wire and 3 mm gaps (supplied by the Environment Agency) as well as a plastic Hydrolox screen section from a rotating band screen consisting of a plastic panel with a grid of holes (Hydrolox, 2024). The flume water was dechlorinated with Prime Dechlorinator and cooled to 17 ± 2 °C with a D—D Aquarium Solution DC 2200. The experiments were recorded with three cameras; a wide-angle camera recording the entire experimental area, a handheld GoPro Hero 9 camera used to record interactions with the screen through the glass flume wall, and a high speed camera recording the screen surface and the adjacent area. The high speed camera had a sampling rate of 80 frames per second to capture the eel's interactions with the screens from above and to conduct kinematic analyses. The flow conditions (shown in Table 1) were established in the flume without screens to have constant flow depth for the length of the working area.

**Table 1**

Experimental treatments showing all combinations of screen type, angle, and bulk velocity that the eels were exposed to in the flume. For the treatment names, the first letter denotes screen type (H = Horizontal Wedge Wire, V = Vertical Wedge Wire, P = Plastic Hydrolox), the number denotes the angle of the screen to the streamwise direction, and any subsequent letter denotes bypass type (FB = Full depth Bypass, BB = Bottom Bypass, SB = Surface Bypass).

Treatment	Screen type	Angle to flow	Bulk Velocity (ms <sup>-1</sup> )	Flow depth (mm)	Bypass
H90	Horizontal	90°	0.15, 0.3	130, 168	No
H31.5	Horizontal	31.5°	0.15, 0.3	130, 168	No
H26.5	Horizontal	26.5°	0.3, 0.45	168, 144	No
H26.5FB	Horizontal	26.5°	0.3, 0.45	168, 144	Yes
H26.5BB	Horizontal	26.5°	0.3, 0.45	168, 144	Yes
H26.5SB	Horizontal	26.5°	0.3, 0.45	168, 144	Yes
H20	Horizontal	20°	0.3, 0.45	168, 144	No
V90	Vertical	90°	0.15, 0.3, 0.56	130, 168, 130	No
V31.5	Vertical	31.5°	0.15, 0.3	130, 168	No
V26.5	Vertical	26.5°	0.3, 0.45	168, 144	No
V20	Vertical	20°	0.3, 0.45	168, 144	No
P90	Hydrolox	90°	0.15, 0.3	130, 168	No

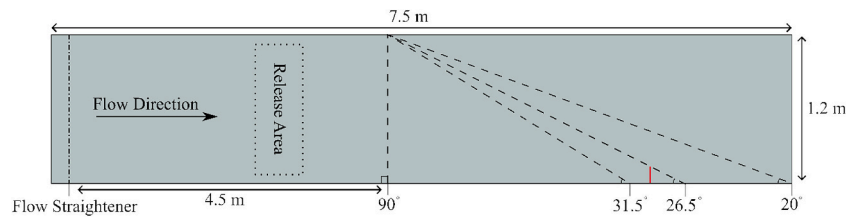


**Fig. 2.** A schematic showing the flume (grey rectangle) with the different angles of channel spanning screens. In treatments where a bypass was present, it was located at the downstream end of the 26.5° screen. The bypass position is indicated by the red line and was 130 mm wide.

### 2.3. Hydrodynamics

Particle Image Velocimetry (henceforth PIV) was used to quantify the flow dynamics of the setup and the screens. PIV was conducted for all screen configurations in both a side view and a top view. The area illuminated by the laser sheet measured 400 mm wide and up to 600 mm long. Where the screen was angled, the equipment was moved across the flume following the screen surface at four locations. For side view PIV, the entire water column was captured, and for top view PIV, three readings were taken, one 20 mm above the bed, one mid-depth, and one 20 mm below the surface water. For all screens and inclinations, the bulk velocities tested for PIV were  $0.15 \text{ ms}^{-1}$ ,  $0.3 \text{ ms}^{-1}$ , and  $0.45 \text{ ms}^{-1}$ , whereas in the eel trials each screen was limited to two bulk velocities. To conduct PIV, a Baumer VLXT-50 M.I camera with a Kowa LM8JC10M 8.5 cm lens was used, recording at 120 frames per second. To produce the laser sheet and synchronise it to the camera, a Rigol 1032Z wave generator was used in conjunction with a Polytec BVS – II Wotan Flash stroboscope at 15 % intensity and a STEMMER IMAGING CVX Triggerbox. The flow was seeded at  $0.063 \text{ gL}^{-1}$  of AXALTA Talisman 30 White 110 particles. All other light sources were temporarily shut off during the PIV recording. The PIV images were recorded as TIFF files and stored on an external hard drive then analysed with PIVlab version 2.63 in MATLAB R2023a. Custom MATLAB scripts were then utilised to further analyse the results of the PIV exported from PIVlab. The streamwise velocity was defined as  $u$ , the vertical velocity as  $w$ , and the lateral velocity as  $v$ , the bulk velocity (spatially and temporally averaged  $u$ ) was called  $U$ , and the temporal fluctuations in streamwise velocity and lateral velocity termed  $u'$  and  $v'$  respectively. The resultant velocity was termed  $R$  ( $\sqrt{u'^2 + v'^2}$ ), the screen angle as  $\alpha$  to the longitudinal direction, and the horizontal Reynolds Shear Stress (RSS) was calculated as  $\tau_{uv} = -\rho(\overline{u'v'})$ . The sweeping velocity ( $V_s$ ) defined as the component of the velocity parallel to the screen and the escape velocity ( $V_e$ ) defined as the component of the velocity perpendicular to the screen were calculated as:

$$V_s = \left( \sqrt{u^2 + v^2} \right) \cos \left( \alpha - \tan^{-1} \frac{v}{u} \right) \quad (1)$$

$$V_e = \left( \sqrt{u^2 + v^2} \right) \sin \left( \alpha - \tan^{-1} \frac{v}{u} \right) \quad (2)$$

### 2.4. Experimental procedure

The trials were conducted in daytime hours and the light sources were kept constant throughout the trials. Of the 32 eels collected, 30 were chosen for the trials and all eels completed all treatments. The eels were acclimated to the flume water for one hour before being exposed to a flow of  $0.15 \text{ ms}^{-1}$  for 15 min prior to the beginning of the trial. At the start of the each trial, the eels were placed upstream of the screen in the release area (Fig. 2) at  $0.15 \text{ ms}^{-1}$  for 5 min and then at  $0.3 \text{ ms}^{-1}$  for a further 5 min for screen angles of  $90^\circ$  and  $31.5^\circ$ , whereas for angles  $26.5^\circ$  and  $20^\circ$ , the first 5 min were spent at  $0.3 \text{ ms}^{-1}$  and the following 5 min at  $0.45 \text{ ms}^{-1}$ . Any trial was interrupted if an eel became impinged, this was defined as a state of exhaustion in which the eel was unable to detach from the screen and swim upstream and was tested by starting a

60 s timer every time an eel rested on a screen. If after 60 s the eel was still in contact with the screen, the back of the screen was tapped to dislodge the eel if it had the strength to swim away, if it remained impinged, it was declared impinged and moved to a recovery tank. If the eel moved away from the screen within the 60 s or after the screen was tapped, it was considered as resting during that time and the experiment was allowed to continue. Any subsequent contact with the screen started a new 60 s timer. If the full 10 min of the experiment elapsed with no impingement, the eel was removed and placed in a recovery tank. In the event of an eel passing downstream of the screen, it was placed upstream again with a fish net, the escape noted, and the experiment was continued. For the vertical wedge wire screen and the Hydrolox screen at  $90^\circ$ , a third bulk velocity of  $0.56 \text{ ms}^{-1}$  was tested for a further 5 min if the fish had not impinged prior, this was done to test the maximum velocity the flume could achieve with those conditions to evaluate if  $0.56 \text{ ms}^{-1}$  was sufficient to reliably impinge the eels in a short time for use in fish recovery and return systems, a full list of treatments and velocities is specified in Table 1. After all trials, each eel was inspected visually for external injuries sustained during the trial. Water temperature of the flume was monitored throughout the day and remained within the specified margin.

### 2.5. Kinematic analysis of the eel screen interaction

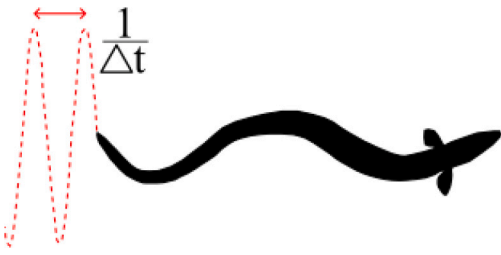


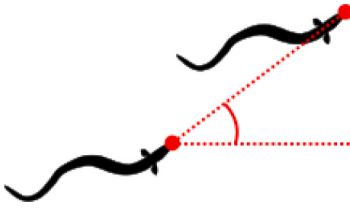
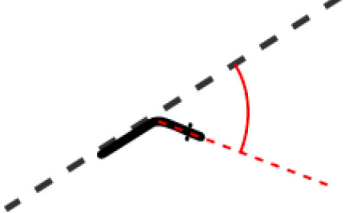
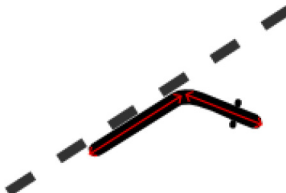
Kinematic videos recorded at 80 frames per second (fps) were analysed in Kinovea (Charmant, 2022). The videos were subjected to a frame-by-frame manual analysis which produced robust data despite small surface wave interference that prevented automated tracking. The full list of tracked parameters is available in Table 2. For a subset of clips, a minimum of equidistant 10 points were tracked along the length of the eel's body to fully visualise the swimming gait and evaluate swimming amplitude.

### 2.6. Statistical analysis

The behavioural and kinematic data were analysed in RStudio R version 4.2.2 (R Core Team, 2022). For generalised linear mixed models (GLMM), which addressed the issue of pseudoreplication by the use of each fish in every treatment, we used nlme and lme4 packages (Bates et al., 2015; Carey and Wang, 2001). For generalised linear models (GLM), the MASS package was used (Venables and Ripley, 2002). For all variables, the effect of the same fish being used in each treatment was evaluated by running a null GLMM and then finding the  $R^2$  value to determine if a GLMM was necessary following established methods (Sonnino Sorisio et al., 2024). This approach revealed that fish id had no effect and GLMs were therefore used because of better model fits. To find the best model, the AIC values and the residuals were inspected, and the best fitting model was chosen. For all models considering the impingement rate and passage rate, a binomial GLM with a cloglog link was used. The analysis of the number of rejections from the eels to the bypass, a poisson GLM was used with a log link. The remainder of the statistical models for behavioural and kinematic variables were gaussian GLMs with identity links except for passage time of eels with bypass design, which was an inverse gaussian GLM with a  $1/\mu^2$  link.

**Table 2**

The kinematic parameters were measured in Kinovea for 80 fps clips. Frame-by-frame analysis was used to track the eels near the screen. The reference direction was always to the longitudinal flow direction and a screen perpendicular to the flow is considered at  $90^\circ$  to the flow.

Variable	Description	Schematic
Tailbeat frequency (Hz)	Frequency of the oscillation of the caudal fin	
Swimming speed ( $BLs^{-1}$ )	The ground speed of the fish plus the flow velocity normalised by fish length when swimming in the upstream direction	
Swimming orientation (deg)	The direction of alignment of the fish's body	
Swimming direction (deg)	The direction of movement of the fish	
Escape angle (deg)	The angle of the fish's body to the screen at the moment of escape from the screen	
Attached proportion (-)	Proportion of the fish's body length touching the screen directly before escape	

### 3. Results

#### 3.1. Hydrodynamics

The flow in the flume with fish screens was characterised by Reynolds numbers between 16,000 and 60,000 (based on hydraulic radius) and was dominated by the streamwise component of the velocity. With a  $90^\circ$  screen, the vertical and lateral velocity components to the velocity were unaffected and the effect of the screen on the flow only reduced the longitudinal velocity within 50 mm upstream of the screen surface. This occurred uniformly across the channel width, only being affected by the wall effects on either side, and these findings remain true for both horizontal and vertical wedge-wire screens. At lower velocities, for both the Hydrolox screen and wedge-wire screens, the impact of the screen on the flow field were similar but at higher velocities there was a more

marked deceleration of the flow in proximity of the Hydrolox screen but not to the extent of modifying the screen performance. At screen angles between  $31.5^\circ$  and  $20^\circ$  to the flow, the velocity remained uniform and there were minor deviations of the flow in the direction of the screen within 30–50 mm of the screen surface, introducing a lateral velocity component, as seen in Fig. 4. Where the screen meets the flume wall (where no bypass is present), there is a reduction in velocity magnitude that is higher with screen angles  $20^\circ$  and  $26.5^\circ$  and lower at a screen angle of  $31.5^\circ$ . Despite the velocity reduction, the velocity gradients remain low, with no harsh transitions in flow regime being present in any screen configuration without a bypass. Consequently, Reynolds Shear Stress (RSS) magnitudes were never elevated, with slightly higher values in higher velocities but no areas of consistently high RSS (Fig. 3).

With a bypass present (with a screen at  $26.5^\circ$  to the flow), the flow fields upstream of the opening remained unaffected, whilst the velocity

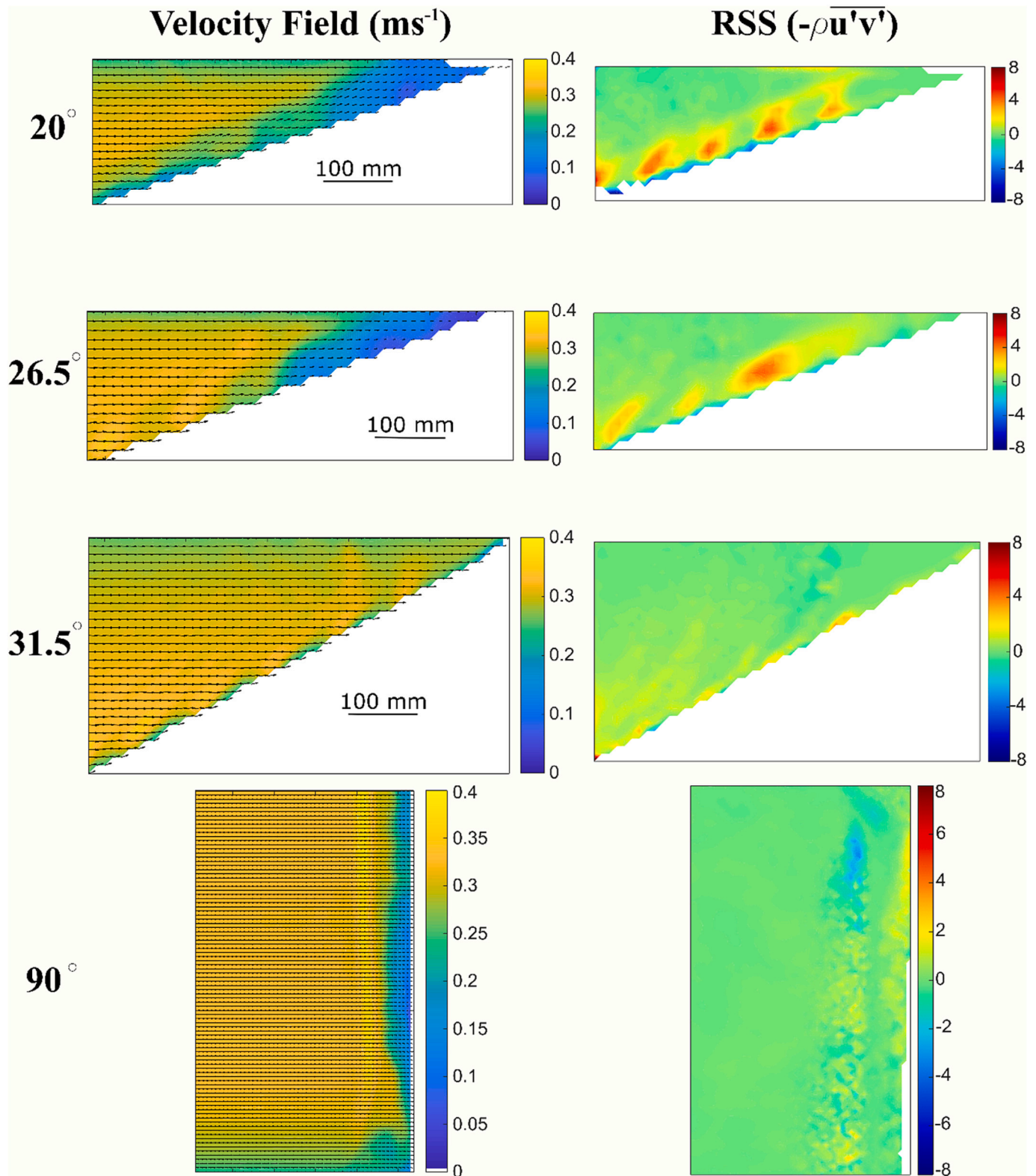
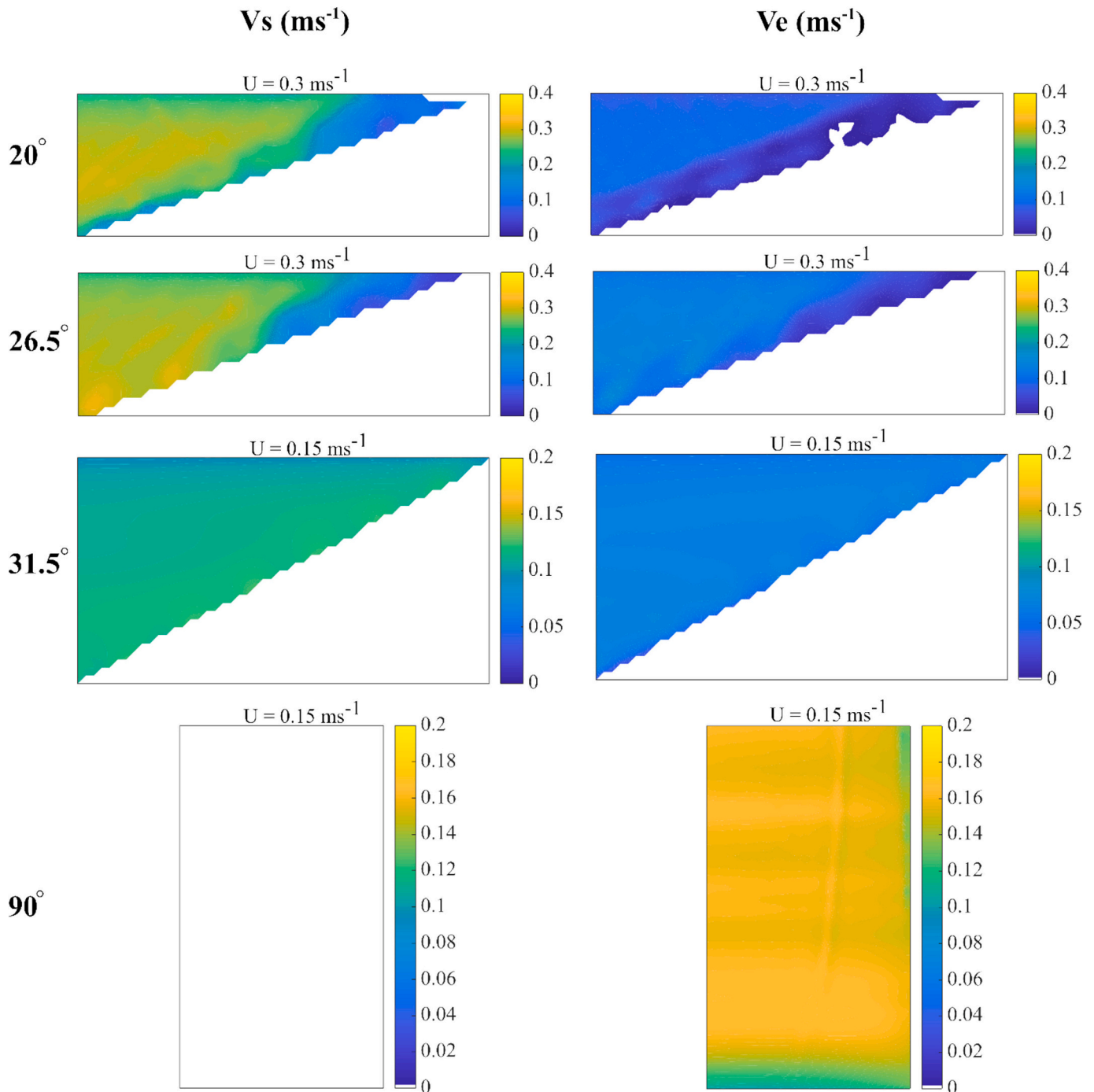


Fig. 3. Top view contour plots showing the resultant velocity, vectors composed of the streamwise and lateral velocity components ( $\text{ms}^{-1}$ ) and horizontal Reynolds Shear Stress (RSS;  $\text{kgm}^{-1} \text{s}^{-1}$ ). All plots are from conditions with  $0.3 \text{ ms}^{-1}$  bulk velocity and for a horizontal wedge-wire screen without bypass. Measurements are taken at mid depth, white areas on plots indicate that no data was available, the streamwise velocity is left to right and the plots are not to scale. For the top six plots, the top boundary is the left hand side flume wall and in the  $90^\circ$  plots top and bottom are both flume walls. Plots for all other flow conditions and screens are in the supplementary materials.

increased when approaching the bypass. The full depth bypass showed a mild velocity gradient leading to the opening and a wake with a few turbulent vortices and lower vorticity values compared to the other bypass types. The bottom and surface bypasses both showed sharper flow accelerations at mid flow depth as a result of half of the flow depth being blocked for the width of the opening. With these two bypasses, enhanced vertical velocities were generated that contributed to the increased velocity gradient. In the wake of the bottom and surface bypasses, for all flow conditions tested, a vortex street was shed from the trailing edge of the screen with areas of high vorticity. Plots and videos

showing these wake characteristics are present in the Appendices.

The sweeping and escape velocities ( $V_s$  and  $V_e$  respectively) as defined in the methods are a measure of how well a screen can guide fish downstream and how difficult it is for fish to swim away from the screen. An analysis of these components of the velocities in Fig. 4 shows how sweeping velocities are greatest for smaller screen angles and decrease to zero for perpendicular screens. The escape velocity, however, shows the opposite trend, being very low at  $20^\circ$  and steadily increasing to a maximum at  $90^\circ$ , where it is approximately the same as the streamwise velocity component. The magnitude of these velocities was driven less



**Fig. 4.** Top view contour plots of sweeping velocity ( $V_s$ ) and escape velocity ( $V_e$ ) for a horizontal wedge-wire screen at the four angles tested. For each angle, the plots portray  $V_s$  and  $V_e$  for the bulk velocity that represents the maximum allowable velocity at the screen according to Environment Agency guidance ( $0.15 \text{ ms}^{-1}$  for screens at  $90^\circ$  and  $31.5^\circ$ , and  $0.3 \text{ ms}^{-1}$  for screens at  $26.5^\circ$  and  $20^\circ$ ). Measurements are taken at mid depth, white areas on plots equate to values equal to 0 or where no data was available. Plots for all velocities tested and screen types are available in the supplementary materials.

by the flow being deviated by the screen (Fig. 3) and mostly by the screen angle as shown by the closeness of the data points in Fig. 5 to plots of sine and cosine, indicating that for the flow conditions tested screen angle governs  $V_s$  and  $V_e$  magnitude. When normalised by the bulk velocity, there is little variation in  $V_s$  and  $V_e$  between different bulk velocities and screen angles, again pointing to the screen angle being dominant over other flow characteristics produced by the screen, making these velocities predictable if screen angle and bulk velocity is known for a uniform cross-sectional channel such as a laboratory flume.

### 3.2. Impingement

For all screens at the maximum permissible flow velocity for that angle according to regulation ( $0.15 \text{ ms}^{-1}$  for screens at  $90^\circ$  and  $31.5^\circ$ , and  $0.3 \text{ ms}^{-1}$  for screens at  $26.5^\circ$  and  $20^\circ$ ), there was no impingement and this was independent of screen type (GLM,  $p > 0.4$ ). Impingement was recorded only in velocities exceeding the regulation velocity, which were set as an ulterior  $0.15 \text{ ms}^{-1}$  beyond the regulation velocity. Higher bulk velocities significantly increased impingement (GLM,  $p < 0.02$ ), and impingement probability increased with velocity, reaching a maximum for the  $0.56 \text{ ms}^{-1}$  condition as shown in Fig. 6A. It should be noted in Fig. 6A that the  $0.3 \text{ ms}^{-1}$  data includes all angles including angles for which  $0.3 \text{ ms}^{-1}$  was the lower velocity and at which no impingement occurred. Impingement was also significantly higher with higher angles (GLM,  $p < 2e-16$ ), with screens perpendicular to the flow having the highest impingement rates. For fish that impinged, it took longer to impinge with the  $90^\circ$  screen (GLM,  $p < 0.035$ ), potentially due to the lower velocities in that treatment at the start of the trials. Despite the low impingement numbers (maximum 20 %, minimum 3 %, overall 9.6 %), 68 % of fish made contact with the screen at least once but could swim upstream in the majority of these contacts.

Throughout the trials, no entrainment occurred through the 3 mm screen gaps, showing that it is an appropriate opening for the size of eels. However, during pre-trial tests if any small gaps were left between the different sections of the screen (since they were made up of between one

and three different sections) or between the screen and the flume bed, eels commonly found these gaps and passed downstream.

### 3.3. Bypasses and passage

In the trials with the different bypass arrangements, there was no significant difference in overall passage rate between bypass types (GLM,  $p > 0.38$ ). Passage time, however, was quicker for the full depth bypass (GLM,  $p < 0.05$ ) but not significantly different between surface and bottom bypasses (GLM,  $p = 0.52$ ) despite the mean passage time being lower for the bottom bypass as shown in Fig. 6B. Fish rejected the surface bypass significantly more often (GLM,  $p < 0.002$ ) than the other bypasses in which very few rejections occurred (Fig. 6C). Fish length did not impact bypass passage nor impingement (GLM,  $p > 0.05$ ).

### 3.4. Kinematics

Behaviour was analysed for all video clips where an eel rested on and escaped from the screen before swimming upstream. The escape angle (Table 2) was significantly higher with higher screen angles (GLM,  $p = 1.8e-15$ ) as the eels point themselves into the flow. The proportion of the body in contact with the screen immediately before escape, however, showed no correlation with screen angle. When approaching the screens, fish were significantly more likely to make contact with the screen head-first when the screen was perpendicular to the flow and tail-first with all other screen angles (GLM,  $p = 2e-16$ ).

Screen angle impacted the body movements made by the eels to escape from the screen after contact or a period of resting. As shown in Fig. 7, the angle the eel must produce between its body and the screen to point itself into the flow is smaller, the smaller the screen angle. The trajectory of the eel post-escape shows how the eels are able to move in a cross-flow direction with the lower angled screens but at  $90^\circ$  they must propel themselves directly against the flow and therefore push off the screen.

The distance the fish swam from the screens correlated with the orientation angle the eels were swimming at (GLM,  $p = 4.7e-15$ ). The swimming direction was also related to the orientation angle of fish swimming (GLM,  $p = 2e-16$ ), the orientation angle being smaller than the overall direction of movement of the fish as they contend with the oncoming flow. The degree to which the eels swam directly against the flow increased in proportion to how large the angle to the flow their trajectory was (GLM,  $p = 6.7e-9$ ), and this appeared to cause the fish to increase their tailbeat frequency (GLM,  $p = 0.02$ ), suggesting increased energy expenditure.

A detailed analysis of the swimming gait of the eels swimming at different angles (Fig. 8) revealed how the amplitude is asymmetric when swimming at an angle to the flow. In Fig. 8B and C where the eel is swimming at increasingly larger angles to the flow, the swimming amplitude on the downstream side of the red trajectory line (left side of Fig. 8B and C) is larger than the upstream. The head amplitude is also increased in 8B compared to the fish swimming in 8A and is largest in 8C. This is consistent with the previous findings of the eel orientation having a smaller angle to the flow than the swimming direction. By comparison, Fig. 8A shows a symmetrical gait with a low head amplitude. The eel is therefore swimming asymmetrically to move at an angle and traverse the flow while still making upstream progress.

## 4. Discussion

This study found that the current England and Wales guidance create an effective protection for eels in the tested size range of 121–300 mm if all guidelines are followed. Importantly however, when velocity was increased, impingement started to occur, and whenever in the pre-trials there was a small gap between screen panels, there were high levels of entrainment. The levels of impingement found in this study are lower than found in a previous study concerning eels with a similar size range,

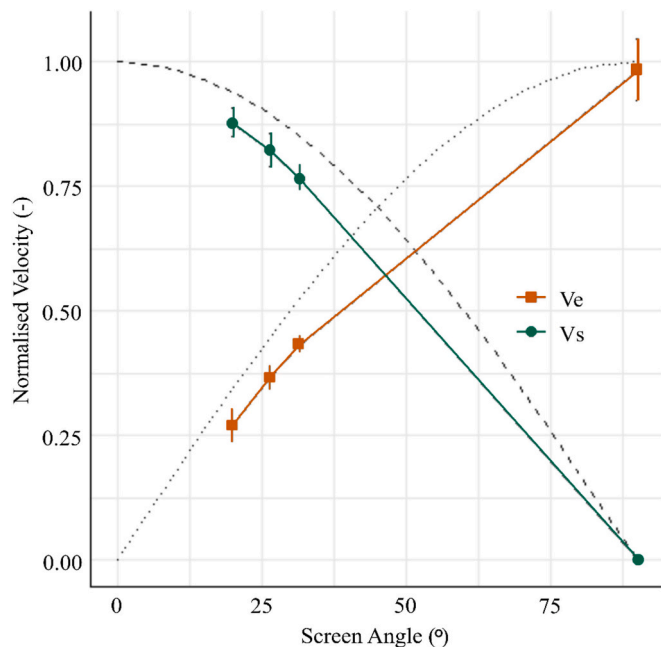
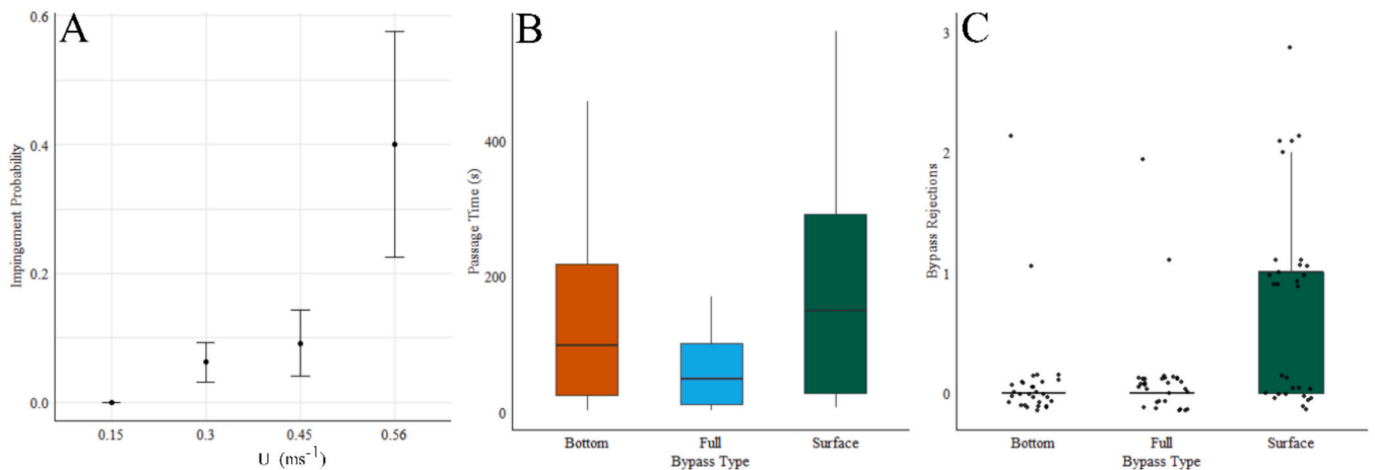
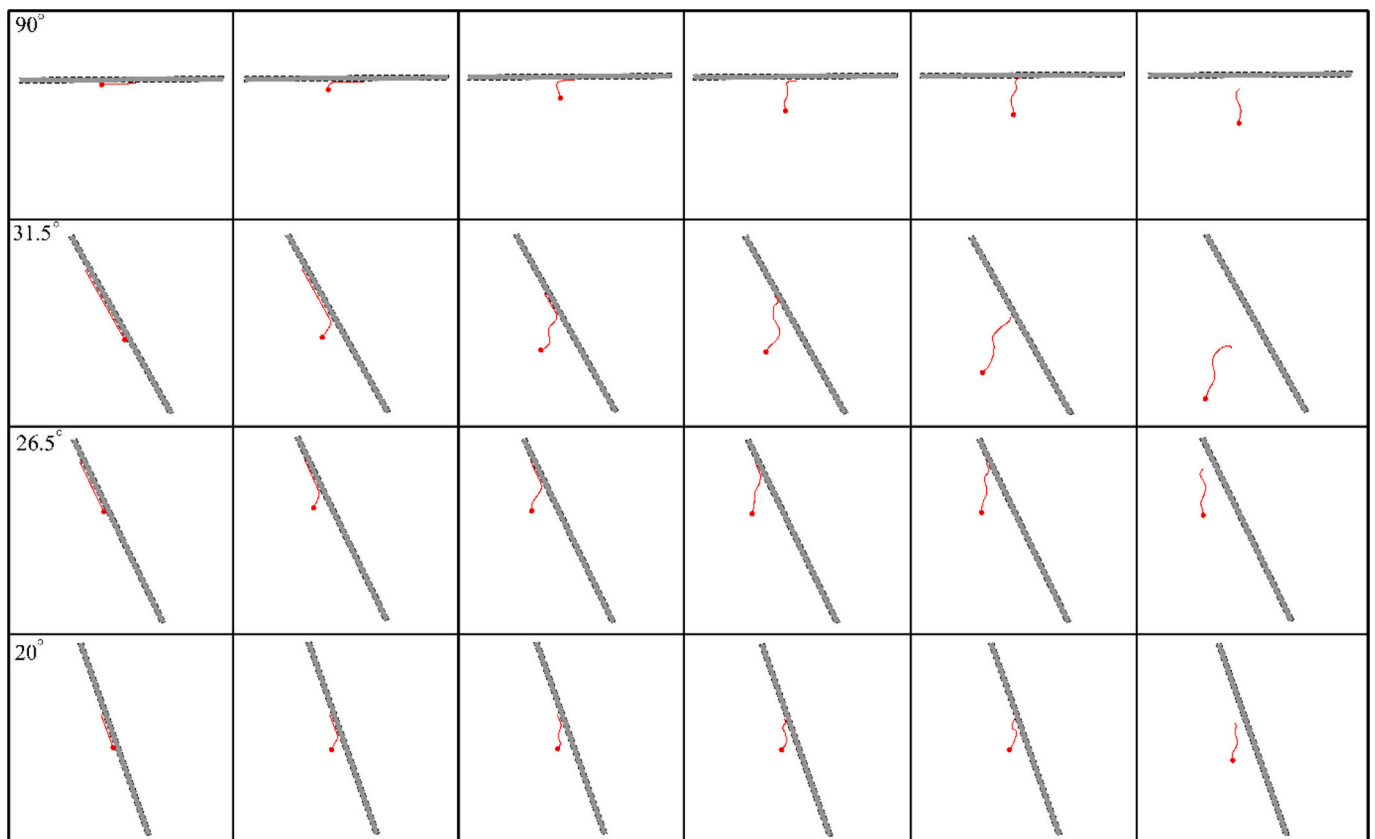


Fig. 5. A plot of the average sweeping ( $V_s$ ) and escape ( $V_e$ ) velocities normalised by bulk velocity ( $U$ ) against screen angle based on a sampling area within 300 mm of the screen surface. For each angle, data from all flow conditions and screen types are combined, their variation is represented by the whiskers on each data point. The dotted and dashed lines represent sine and cosine functions respectively.





**Fig. 6.** A – Impingement probability with bulk velocity ( $U$ ) with standard error bars. It should be noted that in this plot, the 0.3 data contains all angles including those at which 0.3  $\text{ms}^{-1}$  was the lower velocity where no impingement occurred. B – Time taken by the fish to pass downstream using the bypass for each bypass type. C – Number of times each fish rejected the bypass according to bypass type.



**Fig. 7.** Four series of frames showing six stages of fish releasing from the screen at each screen angle tested. The frames are in succession from left to right, starting with the fish flat against the screen. The screen is represented by the grey bar and the fish by the red line with the red circle representing the head. All swimming events portrayed on this plot were taken from trials at 0.3  $\text{ms}^{-1}$  (flowing from bottom to top) for the purposes of comparison and are representative of the manner in which the eels escaped from the screen. Each sequence of frames is taken from a different eel for each treatment and each sequence is drawn from a single clip. (For interpretation of the references to colour in this figure legend, the reader is referred to the web version of this article.)

where impingement occurred at a lower velocity (Carter et al., 2023). This difference in impingement rates can be attributed to differences in methodology and how impingement was defined in the two studies, with this study considering the eels as ‘resting’ if they could subsequently (and within the allowed time of 60 s) escape from the screen whilst they would be considered impinged in the aforementioned study. Using a similar definition of impingement to Carter et al. (2023) would result in

impingement rates of 68 % instead of 9.6 %. The water temperature could also be a contributing factor to the lower impingement, temperature increases swimming speed in fish, allowing them to escape from a screen more easily if the temperature is high (Clough et al., 2004; Muhawenimana et al., 2021). This study found no difference between the two bar orientations of wedge-wire screens, similar to studies using bar racks (de Bie et al., 2021), however, other studies have found

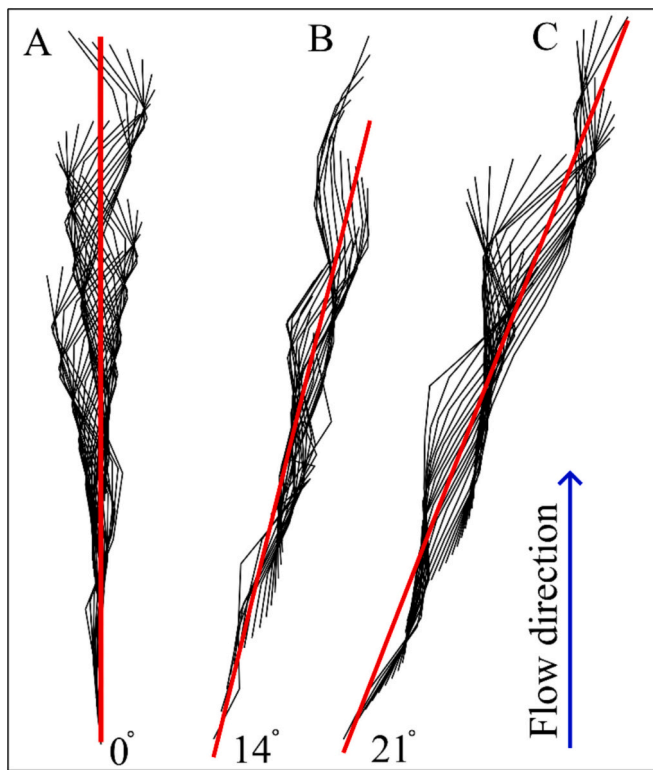


**Fig. 8.** Three plots showing the swimming trajectories and body positions of eels swimming at progressively larger angles to the flow direction. Each black line is the midline of the eel body and successive black lines show progression frame-by-frame of a representative clip of a single eel swimming at an angle to the flow, with the head of the eel facing the bottom of the plot and the water flowing from bottom to top. The red lines show the overall path of the eel. All swimming events portrayed in this plot were taken from trials at  $0.3 \text{ ms}^{-1}$  when the eels were swimming away from the screen. (For interpretation of the references to colour in this figure legend, the reader is referred to the web version of this article.)

differences between horizontal and vertical screens and racks, vertical wedge wire screens have previously been found to produce a higher velocity gradient towards a bypass and therefore decrease chub (*Squalius cephalus*) passage (de Bie et al., 2018). Hydrodynamically, the vertical and horizontal wedge wire produced similar flow fields on a flume scale (Lemkecher et al., 2022).

Screens with smaller angles to the flow reduced impingement rate but for the fish that did impinge, the time before impingement was shorter for perpendicular screens. This can probably be explained by considering that the  $90^\circ$  screen had lower flow velocities than  $20^\circ$  and  $26.5^\circ$  but can also point to the difficulty of releasing from a  $90^\circ$  screen. The kinematics reveal how the eel must first point itself into the oncoming flow, which requires them to turn more for perpendicular screens and less for screens closer to the flow, and then they must push off from the  $90^\circ$  screen directly into the flow whereas with an angled screen they can allow themselves to drift in a crossflow direction before engaging a steady swimming gait (as established by Tytell (2004) and shown in Fig. 8), a manoeuvre which depends less on generating a forward momentum whilst contending with a lower drag force. This hypothesis can potentially explain why fish took longer to impinge with a  $90^\circ$  screen but did so more often; the lower flow velocities allowed the eel to swim upstream of the screen without needing to rest for longer, but once they did make contact with the screen, it was harder to escape from it. To some extent, this phenomenon can also be visualised by considering escape velocity, which is lowest at the smallest angle (shown in Fig. 6). The sweeping and escape velocities, calculated from eqs. 1 and 2, are highly dependent on flow in the streamwise direction

due to the screens not generating comparatively high crossflow velocity components. The sine and cosine lines on Fig. 5 would predict  $V_s$  and  $V_e$  if there was no crossflow ( $v$ ) component, however the screens deviate the flow enough for the measured  $V_e$  and  $V_s$  values to be slightly different but not enough to impact on the fish kinematics. Fig. 8 shows how the eels adapted their swimming gait to diagonal swimming by pointing their bodies at a smaller angle to the flow than their overall movement direction, also meaning that their swimming amplitude is larger on the downstream end of the red line in Fig. 8. This data shows that despite the flow being slightly deviated by the screens, the eels still had to swim against the main longitudinal velocity component ( $U$ ) as well as moving sideways. Where a bypass is present, de Bie et al. (2018) found that  $V_s$  and  $V_e$  increase towards the bypass location, whereas the opposite trend was found in this study when there is no bypass and the screen meets the flume wall. This is due to the flow accelerating towards an open bypass but decelerating if the downstream end of the screen is present (Meister et al., 2020b). The velocity field found at the screens in this study match well with previous literature using ADV (Beck et al., 2020a, 2020b; Meister, 2020; Raynal et al., 2013), and through the use of PIV, velocity fields were measured with higher spatial resolution over a larger sampling area, allowing for the flow to be quantified very close to the screen surface. These detailed readings are particularly useful when considering the flow experienced by impinging fish of small size.

Eels are well known to prefer bottom and full depth bypasses (Calles et al., 2012; Egg et al., 2017; Harbicht et al., 2022; Meister, 2020), although even these can be ineffective. This study found very high passage rates (91 % overall) across all bypass designs, possibly as a result of the modest size of an experimental flume compared to a full scale river meaning that the eels could easily and quickly explore the entire working area. Despite the high passage, there was a distinct difference between passage time for the full depth bypass and the surface and bottom bypasses. This may be attributed to the increased velocity gradient towards the surface and bottom bypasses as half of the flow area is blanked and there is therefore an increase in acceleration towards the open flow area in comparison to the full bypass where the entire area is open. Moderate velocity gradients have been found to increase passage counts whilst harsh ones decrease it (Beck, 2020; Egg et al., 2017; Piper et al., 2015). As a result of the higher velocity present, the surface and bottom bypasses generate a vortex street in the bypass which may deter fish that interact with the vortices (Muhawenimana et al., 2019). The preferred bypass arrangement is therefore the full depth, however this is not always practical to implement in the field. Between the surface and bottom bypasses, the bottom bypass is the best performing option as the eels rejected it far less than the surface bypass (Fig. 6C), this may be due to eels preferring to swim towards the bed of watercourses. It must be noted that the results of these analyses are based on data for which each fish completed every treatment. This effect was partially accounted for using GLMMs, however any learning effects cannot be discounted in this study.

## 5. Conclusion

Lower flow velocities and lower angles to the flow both decrease impingement for 3 mm wedge-wire screens, for which no entrainment occurred, whilst screen orientation did not affect impingement. The angled screen is directly beneficial to the sweeping and escape velocities and allows eels to escape from the screen more easily. This is shown by the kinematic analysis that evidences how the screen angle allows eels to use the sweeping velocity and drift sideways into the open flow instead of needing to overcome the drag on the perpendicular screen. For the three bypass types tested surface, bottom, and full depth bypasses, the full depth is preferable to the bottom bypass, which in turn is better than the surface bypass. The recommended screening techniques in Environment Agency (2020) are appropriate to the tested fish sizes and flow velocities and satisfy the need for fish protection whilst not requiring extremely fine screen aperture, stipulate velocities that are too slow, or

the use of very small screen angles, all of which drive screen and installation price (Clough et al., 2013) thus making these solutions accessible. Of the tested screen types, the passive wedge wire and the Hydrolox screens and orientations performed equally well, however horizontal wedge-wire may be preferable to vertical due to the ease of cleaning as the sweeping velocity could push trash downstream if the screen direction aligns with the velocity.

### CRedit authorship contribution statement

**Guiglielmo Sonnino Sorisio:** Writing – review & editing, Writing – original draft, Visualization, Methodology, Investigation, Formal analysis, Data curation, Conceptualization. **Charlotte Robison-Smith:** Writing – review & editing, Visualization, Methodology, Investigation, Data curation. **Andy Don:** Writing – review & editing, Supervision, Methodology, Funding acquisition, Conceptualization. **Jo Cable:** Writing – review & editing, Supervision, Methodology, Funding acquisition, Conceptualization. **Catherine A.M.E. Wilson:** Writing – review & editing, Supervision, Methodology, Funding acquisition, Conceptualization.

### Declaration of competing interest

The authors declare the following financial interests/personal relationships which may be considered as potential competing interests:

Financial support was provided by Natural Environment Research Council. The authors declare no known competing financial interests or personal relationships that could have appeared to influence the work reported in this paper.

### Acknowledgements

This research was funded by the Natural Environment Research Council (NERC) FRESH CDT grant number NE/R011524/1. Additional resources were provided by the Environment Agency, the screens were provided by the Environment Agency and Hydrolox. The authors thank Paul Greest and Andrew Gott of Natural Resources Wales for providing the eels used in these trials, and Chris Bell and Chris Grzesiok for their advice. We also thank Paul Leech for technical support. The graphical abstract and figure for this paper was created using BioRender.com: Robison-Smith, C. (2025) <https://BioRender.com/g64m566>.

### Appendix A. Supplementary data

Supplementary data to this article can be found online at <https://doi.org/10.1016/j.ecoleng.2025.107547>.

### Data Availability

The data used in this experiment is freely available at doi: [10.17632/bkgws48v3k.1](https://doi.org/10.17632/bkgws48v3k.1).

### References

- Albayrak, I., Maager, F., Boes, R.M., 2020. An experimental investigation on fish guidance structures with horizontal bars. *J. Hydraul. Res.* 58 (3). <https://doi.org/10.1080/00221686.2019.1625818>.
- Bates, D., Mächler, M., Bolker, B.M., Walker, S.C., 2015. Fitting linear mixed-effects models using lme4. *J. Stat. Softw.* 67 (1). <https://doi.org/10.18637/jss.v067.i01>.
- Beck, C., 2020. Fish protection and fish guidance at water intakes using innovative curved-bar rack bypass systems. In: *VAW-Mitteilung*, vol. 257.
- Beck, C., Albayrak, I., Meister, J., Boes, R.M., 2020a. Hydraulic performance of fish guidance structures with curved bars—part 2: flow fields. *J. Hydraul. Res.* 58 (5). <https://doi.org/10.1080/00221686.2019.1671516>.
- Beck, C., Albayrak, I., Meister, J., Peter, A., Selz, O.M., Leuch, C., Vetsch, D.F., Boes, R.M., 2020b. Swimming behavior of downstream moving fish at innovative curved-bar rack bypass systems for fish protection at water intakes. *Water* 12 (11). <https://doi.org/10.3390/w12113244>.

- Behrmann-Godel, J., Eckmann, R., 2003. A preliminary telemetry study of the migration of silver European eel (*Anguilla anguilla* L.) in the River Mosel, Germany. *Ecol. Freshw. Fish* 12 (3). <https://doi.org/10.1034/j.1600-0633.2003.00015.x>.
- Belletti, B., Garcia de Leaniz, C., Jones, J., Bizzi, S., Börger, L., Segura, G., Castelletti, A., van de Bund, W., Aarestrup, K., Barry, J., Belka, K., Berkhuyzen, A., Birnie-Gauvin, K., Bussetini, M., Carolli, M., Consuegra, S., Dopico, E., Feierfeil, T., Fernández, S., Zalewski, M., 2020. More than one million barriers fragment Europe's rivers. *Nature* 588 (7838). <https://doi.org/10.1038/s41586-020-3005-2>.
- Boes, R., Beck, C., Meister, J., Peter, A., Kastinger, M., Albayrak, I., 2022. Effect of Bypass Layout on Guidance of Downstream Moving Fish at Bar Rack Bypass Systems. <https://doi.org/10.3850/iahr-39wc25217192022537>.
- Bromley, R., Coyle, S., Hawley, K., Anderson, K., Turnpenny, A.W.H., 2013. UK Best Practice Fish Screening Trials Study. <https://doi.org/10.2495/978-1-84564-849-7/008>.
- Brown, L., Castro-Santos, T., 2009. Three-Dimensional Movement of Silver-Phase American Eels in the Forebay of a Small Hydroelectric Facility. *Eels at the Edge: Science, Status, and Conservation Concerns*.
- Calles, O., Karlsson, S., Hebrand, M., Comoglio, C., 2012. Evaluating technical improvements for downstream migrating diadromous fish at a hydroelectric plant. *Ecol. Eng.* 48. <https://doi.org/10.1016/j.ecoleng.2011.05.002>.
- Carey, V.J., Wang, Y.-G., 2001. Mixed-Effects Models in S and S-Plus. *J. Am. Stat. Assoc.* 96 (455). <https://doi.org/10.1198/jasa.2001.s411>.
- Carr, J.W., Whoriskey, F.G., 2008. Migration of silver American eels past a hydroelectric dam and through a coastal zone. *Fish. Manag. Ecol.* 15 (5–6). <https://doi.org/10.1111/j.1365-2400.2008.00627.x>.
- Carter, K.L., Reader, J.P., 2000. Patterns of drift and power station entrainment of 0 + fish in the River Trent, England. *Fish. Manag. Ecol.* 7 (5). <https://doi.org/10.1046/j.1365-2400.2000.00224.x>.
- Carter, L.J., Collier, S.J., Thomas, R.E., Norman, J., Wright, R.M., Bolland, J.D., 2023. The influence of passive wedge-wire screen aperture and flow velocity on juvenile European eel exclusion, impingement and passage. *Ecol. Eng.* 192. <https://doi.org/10.1016/j.ecoleng.2023.106972>.
- Charmant, J., 2022. Kinovea (0.9.4). <https://www.kinovea.org/>.
- Clough, S.C., Turnpenny, A.W.H., 2001. *Swimming Speeds in Fish: Phase 1*. Environment Agency.
- Clough, S.C., Lee-Elliott, I.E., Turnpenny, A.W.H., Holden, S.D.J., Hinks, C., 2004. *Swimming Speeds in Fish: Phase 2*. Environment Agency R&D Technical Report W2-049/TR1.
- Clough, S.C., Teague, N., Webb, H., 2013. Even Finer Bar Spacing, how Low Can you Go? <https://doi.org/10.2495/978-1-84564-849-7/005>.
- Council Regulation (EC) No 1100/2007, 2007. *Pub. L. No. 1100/2007*. Off. J. Eur. Union 248, 17–23. <https://eur-lex.europa.eu/legal-content/EN/TXT/PDF/?uri=CELEX:32007R1100>.
- Dainys, J., Stakėnas, S., Gorfine, H., Ložys, L., 2018. Mortality of silver eels migrating through different types of hydropower turbines in Lithuania. *River Res. Appl.* 34 (1). <https://doi.org/10.1002/rra.3224>.
- David, L., Chatellier, L., Courret, D., Albayrak, I., Boes, R.M., 2022. Fish guidance structures with narrow bar spacing: physical barriers. *Novel Dev. Sustain. Hydropower*. [https://doi.org/10.1007/978-3-030-99138-8\\_7](https://doi.org/10.1007/978-3-030-99138-8_7).
- de Bie, J., Peirson, G., Kemp, P.S., 2018. Effectiveness of horizontally and vertically oriented wedge-wire screens to guide downstream moving juvenile chub (*Squalius cephalus*). *Ecol. Eng.* 123. <https://doi.org/10.1016/j.ecoleng.2018.07.038>.
- de Bie, J., Peirson, G., Kemp, P.S., 2021. Evaluation of horizontally and vertically aligned bar racks for guiding downstream moving juvenile chub (*Squalius cephalus*) and barbel (*Barbus barbus*). *Ecol. Eng.* 170. <https://doi.org/10.1016/j.ecoleng.2021.106327>.
- DEFRA, 2022. *ENV15 - Water Abstraction Tables for England*. Department for Environment, Food & Rural Affairs. <https://www.gov.uk/government/statistica/l-data-sets/env15-water-abstraction-tables#full-publication-update-history>.
- Dekker, W., 2003. Status of the European Eel Stock and Fisheries. *Eel Biol.* [https://doi.org/10.1007/978-4-431-65907-5\\_17](https://doi.org/10.1007/978-4-431-65907-5_17).
- Deleau, M.J.C., White, P.R., Peirson, G., Leighton, T.G., Kemp, P.S., 2020a. The response of anguilliform fish to underwater sound under an experimental setting. *River Res. Appl.* 36 (3). <https://doi.org/10.1002/rra.3583>.
- Deleau, M.J.C., White, P.R., Peirson, G., Leighton, T.G., Kemp, P.S., 2020b. Use of acoustics to enhance the efficiency of physical screens designed to protect downstream moving European eel (*Anguilla anguilla*). *Fish. Manag. Ecol.* 27 (1). <https://doi.org/10.1111/fme.12362>.
- Ebel, G., 2016. *Fish Protection and Downstream Passage at Hydropower Plants Handbook of Bar Rack and Bypass Systems, 2nd Ed* (Büro für Gewässerökologie und Fischereibiologie).
- Egg, L., Mueller, M., Pander, J., Knott, J., Geist, J., 2017. Improving European Silver Eel (*Anguilla anguilla*) downstream migration by undershot sluice gate management at a small-scale hydropower plant. *Ecol. Eng.* 106. <https://doi.org/10.1016/j.ecoleng.2017.05.054>.
- Environment Agency, 2020. *Screening at intakes: measures to protect eel and elvers*. LIT, 60516.
- Gosset, C., Travade, F., Durif, C., Rives, J., Elie, P., 2005. Tests of two types of bypass for downstream migration of eels at a small hydroelectric power plant. *River Res. Appl.* 21 (10). <https://doi.org/10.1002/rra.871>.
- Haddington, R.H., Van der Stoep, J.W., Habraken, J.M.P.M., 1992. *Deflecting Eels from Water Inlets of Power Stations with Light*. Irish Fisheries Investigations. Serie A: Freshwater, p. 36.
- Halvorsen, S., Korslund, L., Gustavsen, P., Slettan, A., 2020. Environmental DNA analysis indicates that migration barriers are decreasing the occurrence of European eel

- (*Anguilla anguilla*) in distance from the sea. *Glob. Ecol. Conserv.* 24. <https://doi.org/10.1016/j.gecco.2020.e01245>.
- Hanson, C.H., White, J.R., Li, H.W., 1977. Entrapment and impingement of fishes by power plant cooling-water intakes: an overview. *Mar. Fish. Rev.* 39 (10).
- Harbicht, A.B., Watz, J., Nyqvist, D., Virmaja, T., Carlsson, N., Aldvén, D., Nilsson, P.A., Calles, O., 2022. Guiding migrating salmonid smolts: Experimentally assessing the performance of angled and inclined screens with varying gap widths. *Ecol. Eng.* 174. <https://doi.org/10.1016/j.ecoleng.2021.106438>.
- Haro, A., Castro-Santos, T., Boubee, J., 2000. Behavior and passage of silver-phase American eels, *Anguilla rostrata* (LeSueur), at a small hydroelectric facility. *Dana* 12.
- Holleran, C., 2023. Water Abstraction Statistics: England, 2000 to 2018. Department for Environment, Food and Rural Affairs. <https://www.gov.uk/government/statistics/water-abstraction-estimates/water-abstraction-statistics-england-2000-to-2018#:~:text=In%202018%2C%20the%20most%20recentat%2010.4%20billion%20cubic%20metres>.
- Hydrolox, 2024. Series 1800 Debris Removal/Fish Exclusion Screen.
- ICES, 2020. Joint EIFAAC/ICES/GFCM Working Group on Eels (WGEEEL). *ICES Sci. Rep.* 2 (85). <https://doi.org/10.17895/ices.pub.5982>.
- Jacoby, D., Gollock, M., 2015. *Anguilla anguilla*. *Euro. Eel*. <https://doi.org/10.2305/IUCN.UK.2014-1.RLTS.T60344A45833138.en>.
- Jones, J., Börger, L., Tummers, J., Jones, P., Lucas, M., Kerr, J., Kemp, P., Bizzi, S., Consuegra, S., Marcello, L., Vowles, A., Belletti, B., Verspoor, E., Van de Bund, W., Gough, P., Garcia de Leaniz, C., 2019. A comprehensive assessment of stream fragmentation in Great Britain. *Sci. Total Environ.* 673. <https://doi.org/10.1016/j.scitotenv.2019.04.125>.
- Kirk, R.S., 2003. The impact of *Anguillicola crassus* on European eels. *Fish. Manag. Ecol.* 10 (6). <https://doi.org/10.1111/j.1365-2400.2003.00355.x>.
- Larinier, M., Travade, F., 2002. Downstream Migration: Problems and Facilities. *Bull. Fran. Pêche Piscicult.* 364 (supplément). <https://doi.org/10.1051/kmae/2002102>.
- Lemkecher, F., David, L., Courret, D., Chatellier, L., 2018. Field measurements of the attractiveness of bypasses for fishfriendly trashrack. *E3S Web Conf.* 40. <https://doi.org/10.1051/e3sconf/20184003039>.
- Lemkecher, F., Chatellier, L., Courret, D., David, L., 2022. Experimental study of fish-friendly angled bar racks with horizontal bars. *J. Hydraul. Res.* 60 (1). <https://doi.org/10.1080/00221686.2021.1903587>.
- Meister, J., 2020. Fish Protection and Guidance at Water Intakes With Horizontal Bar Rack Bypass Systems. <https://doi.org/10.3929/ethz-b-000455545>.
- Meister, J., Fuchs, H., Beck, C., Albayrak, I., Boes, R.M., 2020a. Head losses of horizontal bar racks as fish guidance structures. *Water* 12 (2). <https://doi.org/10.3390/w12020475>.
- Meister, J., Fuchs, H., Beck, C., Albayrak, I., Boes, R.M., 2020b. Velocity fields at horizontal bar racks as fish guidance structures. *Water* 12 (1). <https://doi.org/10.3390/w12010280>.
- Motyka, R., Watz, J., Aldvén, D., Carlsson, N., Eissenhauer, F., Harbicht, A., Karathanou, E., Knieps, T., Lind, L., Calles, O., 2024. Downstream passage performance of silver eel at an angled rack: effects of behavior and morphology. *Hydrobiologia*. <https://doi.org/10.1007/s10750-024-05530-5>.
- Muhawenimana, V., Wilson, C.A.M.E., Ouro, P., Cable, J., 2019. Spanwise cylinder wake hydrodynamics and fish behavior. *Water Resour. Res.* 55 (11). <https://doi.org/10.1029/2018WR024217>.
- Muhawenimana, V., Thomas, J.R., Wilson, C.A.M.E., Nefjodova, J., Chapman, A.C., Williams, F.C., Davies, D.G., Griffiths, S.W., Cable, J., 2021. Temperature surpasses the effects of velocity and turbulence on swimming performance of two invasive non-native fish species. *R. Soc. Open Sci.* 8 (2). <https://doi.org/10.1098/rsos.201516>.
- Newbold, L.R., Hockley, F.A., Williams, C.F., Cable, J., Reading, A.J., Auchterlonie, N., Kemp, P.S., 2015. Relationship between European eel *Anguilla anguilla* infection with non-native parasites and swimming behaviour on encountering accelerating flow. *J. Fish Biol.* 86 (5). <https://doi.org/10.1111/jfb.12659>.
- NRW, 2024. Licenced Water Abstractions. DataMapWales. Contains Natural Resources Wales Information © Natural Resources Wales and Database Right. All Rights Reserved. [https://datamap.gov.wales/layers/geonode:nrw\\_water\\_resource\\_permits](https://datamap.gov.wales/layers/geonode:nrw_water_resource_permits).
- Pedersen, M.I., Jepsen, N., Aarestrup, K., Koed, A., Pedersen, S., Økland, F., 2012. Loss of European silver eel passing a hydropower station. *J. Appl. Ichthyol.* 28 (2). <https://doi.org/10.1111/j.1439-0426.2011.01913.x>.
- Pike, C., Crook, V., Gollock, M., 2020. *Anguilla anguilla*, European eel The IUCN Red List of Threatened Species TM. <https://doi.org/10.2305/IUCN.UK.2020>.
- Piper, A.T., Manes, C., Siniscalchi, F., Marion, A., Wright, R.M., Kemp, P.S., 2015. Response of seaward-migrating European eel (*Anguilla anguilla*) to manipulated flow fields. *Proc. R. Soc. B Biol. Sci.* 282 (1811). <https://doi.org/10.1098/rspb.2015.1098>.
- Piper, A.T., Svendsen, J.C., Wright, R.M., Kemp, P.S., 2017. Movement patterns of seaward migrating European eel (*Anguilla anguilla*) at a complex of riverine barriers: implications for conservation. *Ecol. Freshw. Fish* 26 (1). <https://doi.org/10.1111/eff.12257>.
- Piper, A.T., Rosewarne, P.J., Wright, R.M., Kemp, P.S., 2018. The impact of an Archimedes screw hydropower turbine on fish migration in a lowland river. *Ecol. Eng.* 118. <https://doi.org/10.1016/j.ecoleng.2018.04.009>.
- Piper, A.T., White, P.R., Wright, R.M., Leighton, T.G., Kemp, P.S., 2019. Response of seaward-migrating European eel (*Anguilla anguilla*) to an infrasound deterrent. *Ecol. Eng.* 127. <https://doi.org/10.1016/j.ecoleng.2018.12.001>.
- R Core Team, 2022. R: A Language and Environment for Statistical Computing. R Foundation for Statistical Computing, Vienna, Austria. <https://www.R-project.org/>.
- Rajaratnam, N., Katopodis, C., Sadeque, M.A.F., Pokharel, N., 2010. Turbulent Flow near Vertical Angled fish Screen. *J. Hydraul. Eng.* 136 (11). [https://doi.org/10.1061/\(asce\)hy.1943-7900.0000269](https://doi.org/10.1061/(asce)hy.1943-7900.0000269).
- Raynal, S., Chatellier, L., Courret, D., Larinier, M., David, L., 2013. An experimental study on fish-friendly trashracks - part 2. Angled trashracks. *J. Hydraul. Res.* 51 (1). <https://doi.org/10.1080/00221686.2012.753647>.
- Russon, I.J., Kemp, P.S., Calles, O., 2010. Response of downstream migrating adult European eels (*Anguilla anguilla*) to bar racks under experimental conditions. *Ecol. Freshw. Fish* 19 (2). <https://doi.org/10.1111/j.1600-0633.2009.00404.x>.
- Seaby, R., 2023. The impact of mesh size on numbers of fish impinged or entrained in power station cooling water systems. *First Int. Fish Imping. Entrain. Conf.* 49–52.
- Shepherd, M.A., Labay, A., Shea, P.J., Rautiainen, R., Achutan, C., 2016. Operational, water quality and temporal factors affecting impingement of fish and shellfish at a Texas coastal power plant. *Glob. Ecol. Conserv.* 5. <https://doi.org/10.1016/j.gecco.2015.11.006>.
- Sonnino Sorisio, G., Wilson, C.A.M.E., Don, A., Cable, J., 2024. Fish passage solution: European eel kinematics and behaviour in shear layer turbulent flows. *Ecol. Eng.* 203, 107254. <https://doi.org/10.1016/j.ecoleng.2024.107254>.
- Stocks, J.R., Walsh, C.T., Rodgers, M.P., Boys, C.A., 2019. Approach velocity and impingement duration influences the mortality of juvenile Golden Perch (*Macquaria ambigua*) at a fish exclusion screen. *Ecol. Manag. Restor.* 20 (2). <https://doi.org/10.1111/emr.12347>.
- The Eels (England and Wales) Regulations 2009 No. 3344, 2009. The Eels (England and Wales) Regulations 2009 No. 3344. <http://www.defra.gov.uk/foodfarm/fisheries/>.
- Turnpenny, A., O'Keefe, N., 2005. Screening for Intakes and Outfalls: A Best Practice Guide. Environment Agency.
- Turnpenny, A., Blay, S., Carron, J., Clough, S., 2001. Literature Review Swimming Speeds in Fish. [www.environment-agency.gov.uk](http://www.environment-agency.gov.uk).
- Tytell, E.D., 2004. Kinematics and hydrodynamics of linear acceleration in eels, *Anguilla rostrata*. *Proc. R. Soc. B Biol. Sci.* 271 (1557). <https://doi.org/10.1098/rspb.2004.2901>.
- Venables, W.N., Ripley, B.D., 2002. Modern applied statistics with S fourth edition. In: *World*, vol. 53. Springer, New York, NY. <https://doi.org/10.1007/978-0-387-21706-2.7>.
- Veza, P., Libardoni, F., Manes, C., Tsuzaki, T., Bertoldi, W., Kemp, P.S., 2020. Rethinking swimming performance tests for bottom-dwelling fish: the case of European glass eel (*Anguilla anguilla*). *Sci. Rep.* 10 (1). <https://doi.org/10.1038/s41598-020-72957-w>.
- Warren, M.L., Pardew, M.G., 1998. Road crossings as barriers to small-stream fish movement. *Trans. Am. Fish. Soc.* 127 (4). [https://doi.org/10.1577/1548-8659\(1998\)127<0637:rcabts>2.0.co;2](https://doi.org/10.1577/1548-8659(1998)127<0637:rcabts>2.0.co;2).